Pore-Engineered N, S Co-Doped Activated Carbon Decorated with Vanadium Nitride Nanoparticles for Organic Supercapacitors

Zhwan Naghshbandi,[a] Thomas Ebel, [a*]

[a] Centre for Industrial Electronics, Institute of Mechanical and Electrical Engineering, University of Southern Denmark (SDU), Sonderborg, Denmark

*Corresponding author; ebel@sdu.dk

Abstract

A porous N,S co-doped activated-carbon/vanadium-nitride (NS-AC/VN) composite was prepared to combine electric-double-layer charge storage with interfacial and faradaic contributions in an organic supercapacitor electrode. Activated carbon was co-doped with nitrogen and sulfur by thiourea-assisted heat treatment at 700 °C, followed by adsorption of an ammonium metavanadate precursor and ammonolysis to anchor VN nanoparticles on the carbon framework. Field-emission scanning electron microscopy showed that the porous carbon morphology was retained after heteroatom treatment and that fine VN-containing particles were distributed over the modified surface. Symmetric two-electrode cells containing 1 M $TEABF_4$ in acetonitrile were evaluated from 20 Hz to 100 kHz using an LCR meter. At 20 Hz, the NS-AC/VN electrode delivered a series capacitance of 4.16 F and an apparent mass-normalized value of 416 F g^{-1}, while its series resistance was approximately 41 Ω compared with approximately 83 Ω for pristine activated carbon. The simultaneous increase in low-frequency capacitance and decrease in resistance indicate improved ion-accessible charge storage and electrical/interfacial transport.

Keywords: activated carbon; nitrogen–sulfur co-doping; vanadium nitride; organic electrolyte; supercapacitor; frequency response

1. Introduction

The accelerating global transition toward renewable energy sources and electrified transportation has intensified the demand for energy storage technologies capable of bridging the gap between the high energy density of batteries and the high-power density of conventional capacitors [1,2]. Among the various solutions, supercapacitors have attracted substantial scientific and industrial attention owing to their ultrafast charge–discharge kinetics, exceptional cycling stability, wide operating temperature range, and inherent safety advantages over battery-based systems [3].

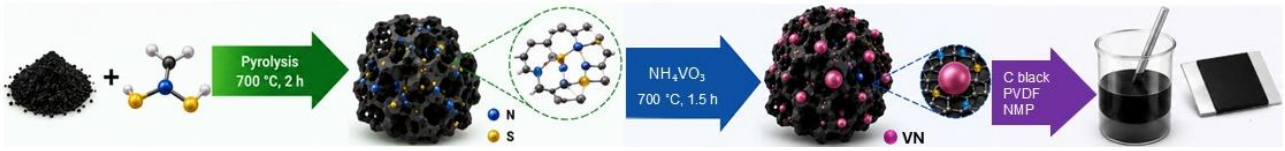
The electrochemical performance of supercapacitors is fundamentally governed by their charge storage mechanism. Electric double-layer capacitors (EDLCs) store charge electrostatically through reversible ion adsorption at the electrode–electrolyte interface, offering excellent power density and cycling stability but limited energy density. Pseudocapacitors, in contrast, rely on fast, reversible surface faradaic redox reactions that deliver higher specific capacitance, often at the expense of long-term stability. Hybrid supercapacitors combine both mechanisms to achieve an improved balance between energy density, power density, and cycle life [4-6]. Recent advances in nanostructured and hybrid composite electrode materials have substantially narrowed the historical energy-density gap between supercapacitors and batteries, enabling higher specific capacitance while preserving rate capability and structural robustness [7,8].

Among electrode materials, activated carbon remains the most widely used choice for EDLC-type supercapacitors due to its low cost, high specific surface area, tunable porosity, and good chemical stability. However, it's purely capacitive charge storage, limited electrolyte wettability, and largely inaccessible microporosity often restricts its practical specific capacitance and rate performance [9-11]. Heteroatom doping has proven an effective strategy to address these limitations. In particular, co-doping activated carbon with nitrogen and sulfur heteroatoms enhances its pseudocapacitive activity, wettability, and electrical conductivity, thereby improving overall charge storage performance, with nitrogen introducing additional redox-active sites and sulfur further improving electrolyte accessibility [12-14].

To further increase energy density, transition metal nitrides such as vanadium nitride (VN) have emerged as promising electrode candidates. VN combines metallic-like electrical conductivity with multiple accessible oxidation states ($V^{2+}/V^{3+}/V^{4+}/V^{5+}$) that enable fast, reversible faradaic reactions and substantial pseudocapacitance, while remaining stable across a wide potential window compatible with both aqueous and organic electrolytes [15-17]. However, VN nanoparticles alone tend to aggregate and suffer from limited long-term cycling stability. Anchoring VN nanoparticles onto a porous, heteroatom-doped carbon matrix helps prevent aggregation, improves structural integrity, and promotes efficient electron transfer between the two components [18,19].

Despite the individual merits of pore-engineered activated carbons and VN-based pseudocapacitive materials, their rational integration with N,S co-doping remains insufficiently explored for organic-electrolyte supercapacitors. In this work, we design and fabricate a porous N,S co-doped activated carbon decorated with VN nanoparticles and evaluate its morphology and frequency-domain response

in a symmetric cell containing $TEABF_4$/ACN. The study focuses on how heteroatom-modified carbon and VN-containing surface domains influence low-frequency capacitance and series resistance relative to pristine activated carbon.



2. Experimental

2.1. Chemicals

Activated carbon (AC), thiourea, ammonium metavanadate (NH_4VO_3) as the vanadium precursor, N-methyl-2-pyrrolidone (NMP)و carbon black, polyvinylidene fluoride (PVDF) as the binder, Tetraethylammonium tetrafluoroborate (TEABF4), and Acetonitrile (ACN) were purchased from Sigma Aldrich and Fisher Scientific used as received without further purification.

2.2. Synthesis of N, S Co-Doped Activated Carbon (NS-AC)

Activated carbon and thiourea were mixed at a weight ratio of 1:1 and thoroughly ground to obtain a homogeneous mixture. The mixture was transferred into a tubular furnace and subjected to heat treatment under a continuous flow of nitrogen at 700 °C for 2 h, with a heating rate of 5 °C/min. After natural cooling to room temperature, the resulting product was washed with deionized water and dried at 80 °C overnight to yield N, S co-doped activated carbon (NS-AC).

2.3. Anchoring of Vanadium Nitride Nanoparticles (Synthesis of NS-AC/VN)

In a typical procedure, 1.0 g of the pore-engineered NS-AC was dispersed in a solution containing 0.25 g of NH_4VO_3 dissolved in a water/ethanol mixture, and the suspension was stirred continuously to ensure uniform adsorption of the vanadium precursor onto the carbon surface. The resulting mixture was dried at 80 °C to completely remove the solvents. The dried precursor was then calcined under a mixed flow of ammonia and nitrogen at 700 °C for 1.5 h with a heating rate of 5 °C/min. After natural cooling to room temperature, the resulting product was washed with deionized water and dried at 80 °C overnight to yield vanadium nitride (VN) nanoparticles anchored on the NS-AC framework.

2.4. Electrode Preparation and Electrochemical Testing

Working electrodes were prepared by mixing NS-AC/VN (75 wt%) as the active material, carbon black (10 wt%) as the conductive additive, and PVDF (5 wt%) as the binder in N-methyl-2-pyrrolidone (NMP) to form a homogeneous slurry. The slurry was coated onto aluminum foil current collectors and pressed to obtain uniform electrodes. The as-prepared electrodes were dried at 100 °C under vacuum overnight prior to electrochemical testing. The electrochemical performance of the resulting electrodes was subsequently evaluated in both aqueous and organic electrolyte systems.

3. Results and discussion

3.1. Morphology

The morphological evolution of the electrode material at each synthesis stage was investigated by field-emission scanning electron microscopy (FE-SEM), as presented in Figure 1. The pristine activated carbon (Figure 1a) displays a characteristic porous and irregular architecture, featuring a rough, heterogeneous surface interspersed with abundant micro- and mesoscale pores and cavities. This hierarchically porous framework offers well-interconnected channels that facilitate efficient electrolyte infiltration and rapid ion transport throughout the bulk of the material, which is a prerequisite for achieving high-rate electrochemical performance. Upon N, S co-doping (Figure 1b), the intrinsic porous skeleton of the activated carbon is largely retained, confirming the structural robustness of the framework under the doping treatment. Nevertheless, a discernible increase in surface roughness and defect density is observed, which can be attributed to the incorporation of heteroatoms into the carbon lattice, disrupting the local atomic ordering and generating additional edge and defect sites. These structural perturbations are expected to enlarge the density of electrochemically accessible active sites and to strengthen the interfacial interaction between the electrode surface and electrolyte ions, thereby promoting both charge-transfer kinetics and pseudocapacitive contributions. Upon the incorporation of vanadium nitride (Fig. 1c,d), fine particles are observed to be distributed over the N,S-doped carbon surface. The intimate contact between the VN particles and the N,S-doped activated carbon is expected to provide continuous electron transport pathways and facilitate ion diffusion through the porous network. This hierarchical porous morphology, together with the homogeneous distribution of VN nanoparticles, is beneficial for increasing the electrochemically active surface area and enhancing the charge storage capability of the composite electrode.

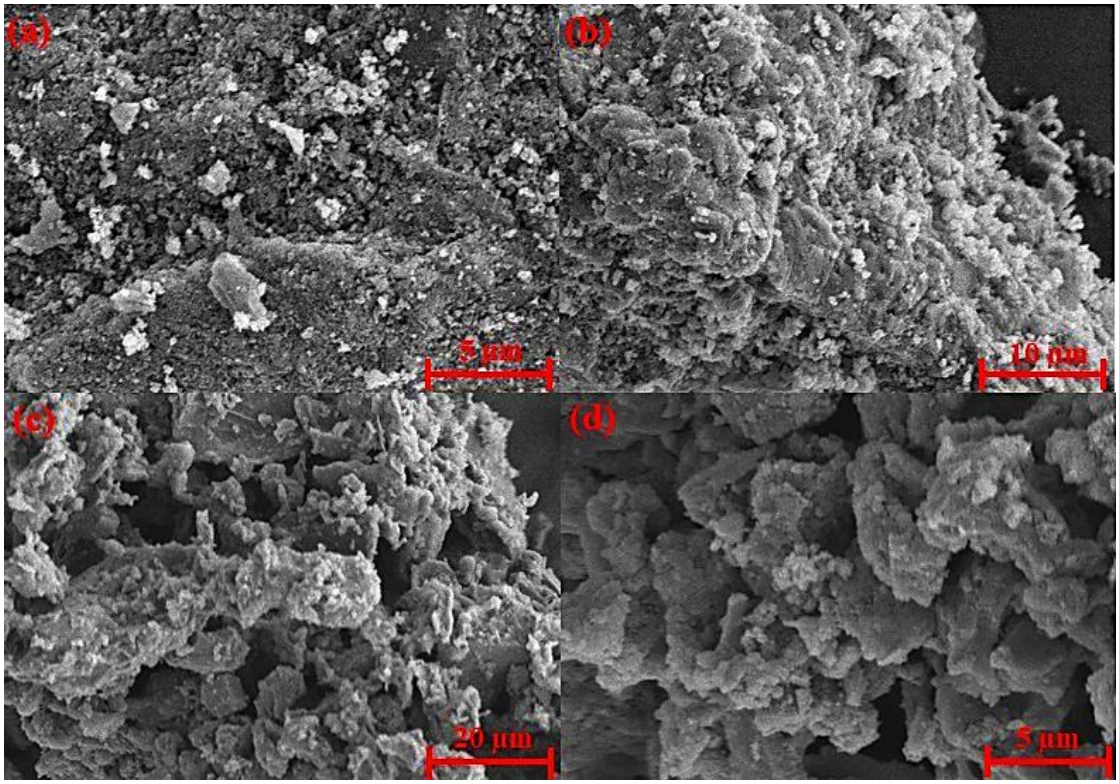


Figure 1. SEM images of (a) pristine activated carbon (AC), (b) N,S co-doped activated carbon (N,S-AC), and (c,d) N,S-AC/VN composite at different magnifications.

3.2. Frequency-Domain Electrochemical Performance in an Organic Electrolyte

The frequency-dependent capacitive behavior of pristine activated carbon (AC) and N,S co-doped activated carbon decorated with vanadium nitride (NS-AC/VN) was investigated in an organic electrolyte using an LCR meter in the series capacitance–resistance (C_s-R_s) configuration over the frequency range of 20 Hz–100 kHz. The measurements were performed using a symmetric two-electrode configuration with **$TEABF_4$/acetonitrile (ACN)** as the electrolyte. As shown in Fig. 2, the NS-AC/VN-based cell exhibited a substantially higher capacitive response than the pristine AC-based cell, particularly in the low-frequency region.

At 20 Hz, the NS-AC/VN cell exhibited a series capacitance (C_s) of 4.16 F. The measured capacitance was normalized with respect to the active-material mass of one electrode (10 mg) according to:

$$C_m = C_s/m$$

Where C_m is the mass-normalized capacitance (F g^{-1}), C_s is the measured series capacitance (F), and m is the active-material mass of one electrode (g). Thus, a mass-normalized capacitance of approximately 416 F g^{-1} was obtained for NS-AC/VN at 20 Hz under the stated single-electrode-mass normalization convention.

frequencies, the longer response time allows electrolyte ions to access a larger fraction of the porous electrode structure and contributes to charge storage. In contrast, at higher frequencies, the shorter response time limits ion transport into less accessible pores, leading to a reduction in the measured capacitance. This frequency dependence is consistent with the expected response of porous carbon-based capacitive electrodes.

The substantially higher capacitance of NS-AC/VN compared with pristine AC indicates that N,S functionalization followed by VN incorporation significantly enhances the capacitive response in the organic electrolyte. The heteroatom-containing surface functionalities may improve electrode–electrolyte interactions and ion accessibility, while VN incorporation may facilitate electrical transport and introduce additional interfacial charge-storage contributions.

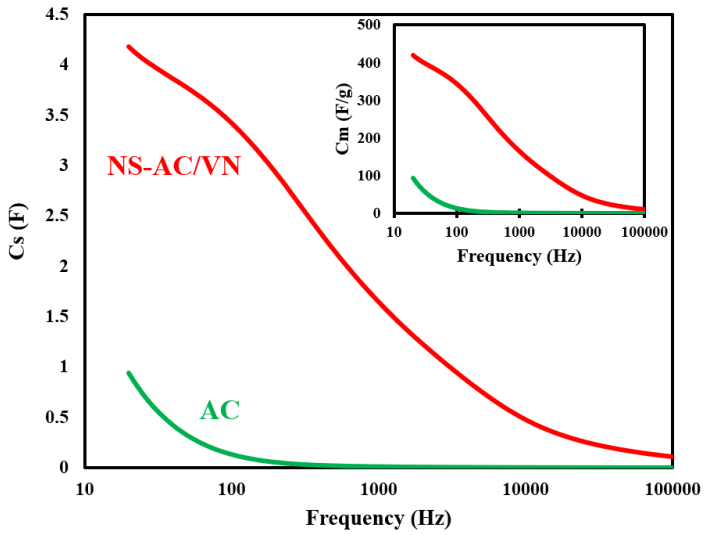


Figure 2. Frequency-dependent series capacitance (C_s) of AC and NS-AC/VN symmetric cells measured in $TEABF_4$/ACN organic electrolyte over the frequency range of 20 Hz–100 kHz. The inset shows the corresponding mass-normalized capacitance (C_m), calculated using the active-material mass of one electrode (10 mg).

The frequency-dependent series resistance (R_s) of the AC and NS-AC/VN cells in the organic electrolyte is presented in Fig. 3. Both samples exhibited a decrease in R_s with increasing frequency;

however, a pronounced difference was observed between the pristine and modified electrodes. At approximately 20 Hz, the AC cell exhibited a series resistance of about 83 Ω, whereas the NS-AC/VN cell showed a considerably lower value of approximately 41 Ω. Thus, the incorporation of N,S functionalities and VN resulted in an approximately two-fold reduction in the low-frequency series resistance.

The difference became even more pronounced with increasing frequency. While the resistance of the pristine AC cell decreased gradually and remained relatively high even in the high-frequency region, the R_s of NS-AC/VN decreased rapidly and approached a substantially lower value at high frequencies. This behavior suggests improved electrical and interfacial transport characteristics in the modified electrode. The lower series resistance of NS-AC/VN may be associated with improved electronic conduction pathways following VN incorporation, together with enhanced electrode–electrolyte interfacial characteristics induced by N,S functionalization.

Importantly, the resistance results are consistent with the capacitance response, where NS-AC/VN exhibited a substantially higher C_s, reaching 4.16 F at 20 Hz. The simultaneous enhancement in capacitance and reduction in series resistance indicates that the N,S functionalization and VN incorporation significantly improve the frequency-dependent electrical response of the activated-carbon-based cell in the organic electrolyte.

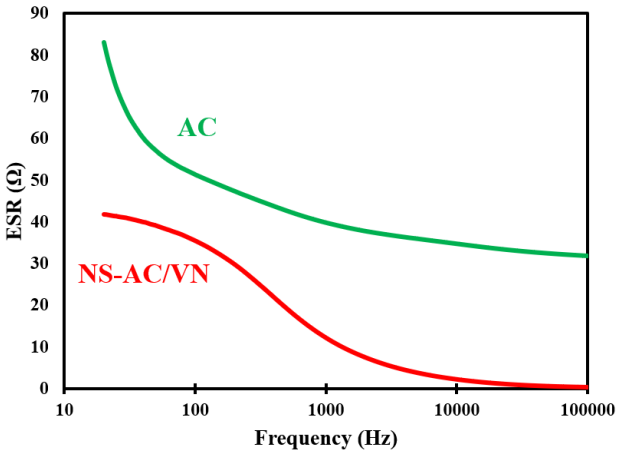


Figure 3. Frequency-dependent series resistance (R_s) of pristine AC and NS-AC/VN cells measured in the organic electrolyte over the frequency range of 20 Hz–100 kHz.

Table 1 compares the capacitive response of the present NS-AC/VN system with representative carbon-based supercapacitors investigated in $TEABF_4$/ACN-based organic electrolytes [20-22]. The

NS-AC/VN cell exhibited a series capacitance of 4.16 F at 20 Hz, corresponding to a mass-normalized capacitance of approximately 416 F g^{-1} under the adopted single-electrode-mass normalization convention. The magnitude of the observed response is encouraging compared with previously reported porous and heteroatom-modified carbon systems operated in organic electrolytes. Nevertheless, direct quantitative comparison should be treated with caution because the present capacitance was obtained from frequency-dependent LCR measurements, whereas most literature values were determined using galvanostatic charge–discharge measurements. Differences in cell configuration, active-material loading, electrolyte composition, voltage window, and normalization methodology may also substantially influence the reported capacitance values.

Table 1. Comparison with carbon-based supercapacitors operated in organic electrolytes.

Electrode Material	Electrolyte	Cm (F/g)	Test condition	Ref.
N-doped reduced graphene oxide (20-N-rGO)	0.2 M PPD + 1 M $TEABF_4$/ACN	340	1 A g^{-1}, pouch cell	20
Activated carbon from biomass	1 M $TEABF_4$/ACN	42.3	symmetric coin cell, 1 A g^{-1}	21
N-doped porous graphene nanoparticles	1 M $TEABF_4$ organic electrolyte	46.5	symmetric coin cell, 0.5 A g^{-1}	22
NS-AC/VN – This work	**1 M $TEABF_4$/ACN**	**416**	**LCR, 20 Hz**	**-**

4. Conclusions

A porous NS-AC/VN composite was produced through thiourea-assisted N,S co-doping followed by precursor impregnation and ammonolysis. FE-SEM observations indicate retention of the porous carbon framework and distribution of fine particles over the modified surface. In symmetric cells containing 1 M $TEABF_4$/ACN, the composite exhibited a substantially larger low-frequency series capacitance and approximately half the series resistance of pristine AC at 20 Hz. These results support the proposed synergy between the accessible carbon network, heteroatom-modified interfaces, and conductive VN-containing domains.

Reference

[1] S. Zhang, N. Pan, Supercapacitors performance evaluation, Advanced Energy Materials, 5 (2015) 1401401.

[2] D.V. Chernysheva, N.V. Smirnova, V.P. Ananikov, Recent trends in supercapacitor research: sustainability in energy and materials, ChemSusChem, 17 (2024) e202301367.

[3] S. Karthikeyan, B. Narenthiran, A. Sivanantham, L.D. Bhatlu, T. Maridurai, Supercapacitor: Evolution and review, Materials Today: Proceedings, 46 (2021) 3984-3988.

[4] G. Jeanmairet, B. Rotenberg, M. Salanne, Microscopic simulations of electrochemical double-layer capacitors, Chemical reviews, 122 (2022) 10860-10898.

[5] W. Raza, F. Ali, N. Raza, Y. Luo, K.-H. Kim, J. Yang, S. Kumar, A. Mehmood, E.E. Kwon, Recent advancements in supercapacitor technology, Nano Energy, 52 (2018) 441-473.

[6] F. Naseri, S. Karimi, E. Farjah, E. Schaltz, Supercapacitor management system: A comprehensive review of modeling, estimation, balancing, and protection techniques, Renewable and Sustainable Energy Reviews, 155 (2022) 111913.

[7] Y. Wang, X. Wu, Y. Han, T. Li, Flexible supercapacitor: Overview and outlooks, Journal of Energy Storage, 42 (2021) 103053.

[8] K. Sharma, A. Arora, S.K. Tripathi, Review of supercapacitors: Materials and devices, Journal of Energy Storage, 21 (2019) 801-825.

[9] M. Islam, M.S. Hossain, B. Adak, M.M. Rahman, K. kubra Moni, A.S. Nur, H. Hong, H. Younes, S. Mukhopadhyay, Recent advancements in carbon-based composite materials as electrodes for high-performance supercapacitors, Journal of Energy Storage, 107 (2025) 114838.

[10] L. Miao, Z. Song, D. Zhu, L. Li, L. Gan, M. Liu, Recent advances in carbon-based supercapacitors, Materials Advances, 1 (2020) 945-966.

[11] N. Choudhary, C. Li, J. Moore, N. Nagaiah, L. Zhai, Y. Jung, J. Thomas, Asymmetric supercapacitor electrodes and devices, Advanced Materials, 29 (2017) 1605336.

[12] F. Wang, N. Samartzis, T. Wang, S. Dai, Synthetic Porous Carbons for High-Energy, High-Power Supercapacitors, Chemical Reviews, (2026).

[13] W. Si, J. Zhou, S. Zhang, S. Li, W. Xing, S. Zhuo, Tunable N-doped or dual N, S-doped activated hydrothermal carbons derived from human hair and glucose for supercapacitor applications, Electrochimica acta, 107 (2013) 397-405.

[14] A. Alabadi, X. Yang, Z. Dong, Z. Li, B. Tan, Nitrogen-doped activated carbons derived from a co-polymer for high supercapacitor performance, Journal of Materials Chemistry A, 2 (2014) 11697-11705.

[15] P. Hu, P. Hu, T.D. Vu, M. Li, S. Wang, Y. Ke, X. Zeng, L. Mai, Y. Long, Vanadium oxide: phase diagrams, structures, synthesis, and applications, Chemical Reviews, 123 (2023) 4353-4415.

[16] Y. Yan, B. Li, W. Guo, H. Pang, H. Xue, Vanadium based materials as electrode materials for high performance supercapacitors, Journal of Power Sources, 329 (2016) 148-169.

[17] D. Ma, C. Han, B. Liu, J. Chen, M. Wu, D. Guan, Vanadium oxide-based electrode materials for advanced supercapacitors: a review, Energy & Fuels, 38 (2024) 10494-10516.

[18] J. Banerjee, K. Dutta, An overview on the use of metal vanadium oxides and vanadates in supercapacitors and rechargeable batteries, International Journal of Energy Research, 46 (2022) 3983-4000.

[19] A.I. Inamdar, S.A. Patil, S.H. Mujawar, A.S. Salunke, S.H. Sutar, N.K. Shrestha, S. Lee, S. Cho, Recent Progress of Vanadium Oxide and its Hybrid Composites-Based Electrochromic Supercapacitors: An Advanced Future Energy Storage Technology, Small, 21 (2025) e09336.

[20] D. Wang, G. Fang, G. Geng, J. Ma, Unique porous carbon constructed by highly interconnected naonowalls for high-performance supercapacitor in organic electrolyte, Materials Letters, 189 (2017) 50-53.

[21] D. Navaneethan, S. Krishna, D. Elumalai, S. Radhakrishnan, K. Kavitha, Activated carbon derived from wood-decaying fungi and their excellent electrochemical performance of organic electrolyte based coin-cell device, Diamond and Related Materials, 157 (2025) 112480.

[22] P.E. Sabzi, A. Rashidi, F. Pourfayaz, A.A.S. Ghazvini, A. Rahimi, E. Akbarinezhad, F. Dehghan, Synthesis and electrochemical performance of pristine and nitrogen-doped porous graphene nanoparticles for high-performance supercapacitors in aqueous and organic electrolytes, Journal of Energy Storage, 167 (2026) 122295.

QUARTZ-S: SMT Electromechanical Relay ESA Qualification

6th Space Passive Component Days (SPCD), International Symposium

13-16 October 2026
ESA/ESTEC, Noordwijk, The Netherlands

Martin Berry[(1)]

[(1)]RADIALL IDA
15 Rue de la Garenne,
38070 Saint-Quentin-Fallavier
Email: martin.berry@radiall.com

ABSTRACT

The constant challenge for space manufacturers is to save both weight and volume. Every gram matters, every cubic centimeter counts. Systems must become more compact and lighter while meeting the uncompromising reliability standards required for space missions. At the same time, cost efficiency remains a key driver in an increasingly competitive industry.

Electromechanical RF switches are widely used in payloads, particularly for redundancy architectures where reliability is absolutely critical. Designers are therefore constantly seeking solutions that maintain the highest levels of performance while reducing cost, weight, and integration complexity.

In response to this challenge, Radiall developed five years ago an innovative SMT electromechanical RF switch, designed to integrate the switching function directly onto the PCB. By eliminating traditional coaxial RF ports, this solution enables a new level of compactness and system integration. The device weighs less than 10 grams, compared to approximately 60 grams for conventional solutions. Even more significant are the system-level savings achieved by replacing RF cable assemblies with direct PCB track interconnections.

The first qualification campaign was successfully completed in 2022. Following this milestone, the focus shifted toward industrialization in order to prepare the product for repeatable and reliable series production. Several batches of flight models have since been manufactured. As is often the case in such programs, this phase allowed us to refine manufacturing processes, improve tooling performance, and strengthen overall process robustness.

Today, the product has reached a new maturity level and we are ready to freeze the design and manufacturing baseline in preparation for ESA QPL qualification.

This presentation will first revisit the operating principles of these SMT electromechanical switches, and then detail the development, industrialization, and qualification journey that has brought us to this key milestone.

As of March 10th, the qualification test campaign has just begun. The schedule is secured, and completion is expected within the planned timeframe. We are therefore confident that this work will soon stand as a compelling success story to be presented at the 2026 SPCD conference.

INTRODUCTION

In 2020, Radiall was included in SELECTOR consortium, “Smt compatible ELECTroMechanical relay for cOmpact redundancy Ring”

SELECTOR value chain includes a supplier of space passive component “Radiall”, a space integrator “Thales Alenia Space”, a leader into electromagnetic design the “Universitat polytecnica of Valencia” and a center of excellence for space reliability of high complexity miniature component the “CSEM”.

SELECTOR initial objective was to reinforce European technological autonomy by developing innovative passive components for the space sector. The project focuses on high miniaturization through SMT-compatible electromechanical relays (MEMR), with the objective to add them to ESA’s European Preferred Part List (EPPL) for unrestricted industry-wide access.

Strategic Goal: Reduce EU’s technology dependence and strengthen European space industry competitiveness.

Developments:

- To have Space-qualified, SMT-compatible Miniature Electromechanical Relays (MEMR), already validated in terrestrial microwave applications.
- To include it in the ESA EPPL to ensure availability to all European manufacturers with no export restrictions.
- To demonstration of a new concept for self-redundant microwave “Metaequipment,” using SMT board-level integration with MEMRs to lower cost and maximize miniaturization.

Target Applications: Very High Throughput Satellites (VHTS), where massive RF chain integration via digital technologies requires cost-driven, miniaturized, highly integrated solutions.

Project ended successfully with the Quartz-S final prototypes qualification and design validation.

OPERATING PRINCIPLE OF THE SMT ELECTROMECHANICAL SWITCH QUARTZ-S

Quartz-S is the commercial name for a latching, SMT, SPDT switch that can work with 6V; 12V or 24V. The only change required to go from one nominal voltage to another is to update the coil wiring.



Fig. 1 Photo of the QUARTZ-S SMT electromechanical switch

The RADIALL electromechanical switches use an arrangement of rectangular coaxial transmission lines either in «transmission line» position or in «isolated line» position to realize the required switching function.

The RF signal is supplied on the input port through the RF connector soldered on a PCB: circular coaxial transmission line; then from the input to the output RF connector antennas, the RF signal is transmitted through the RF cavity via the RF blade in “transmission position”: rectangular coaxial transmission line.

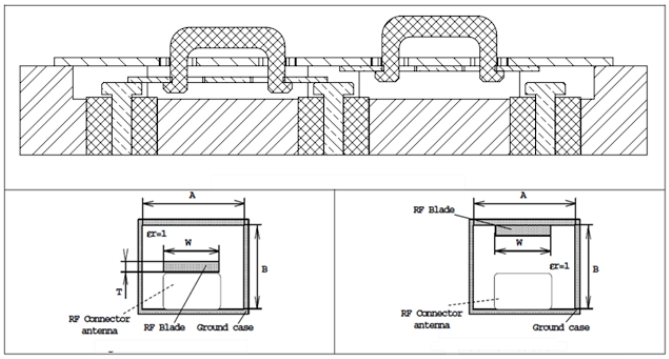


Fig. 2 - RF transmission and isolated lines (simplified view)

The Quartz-S is designed to transmit signal up to 32 GHz. For Qualification testing, the Quartz-S is soldered on a Test fixture with stripline technology and soldered SMA2.9 connector for RF measurement (See “Fig. 3”). Due to this large wideband, there is some difficulty to have test fixture compliant up to 32 GHz. Measurement start to deteriorate after 28 GHz, with TDR analysis, it is confirmed that the performance degradation comes from the test fixture.

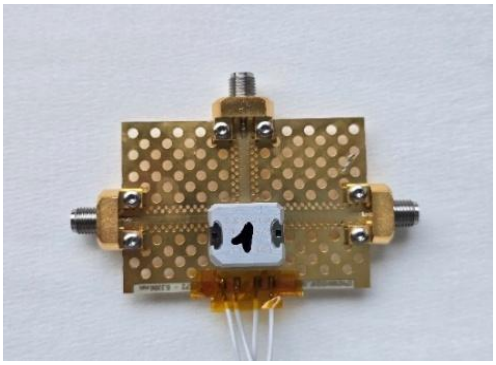


Fig. 3 Photo of the QUARTZ-S Soldered on a test fixture

Insertion Loss and VSWR data measured on qualification unit are given in “Fig. 4” below:

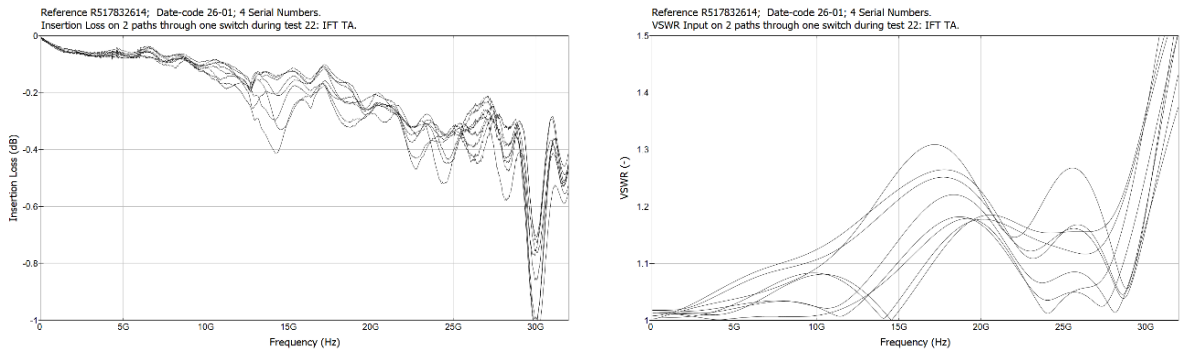


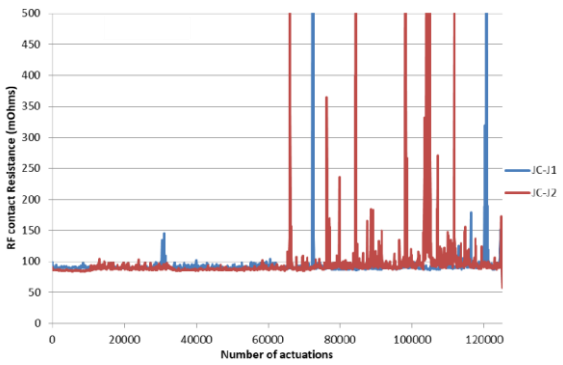
Fig. 4 Qualification initial IL & VSWR performance DC-32 GHz (4 units)

DEVELOPMENT AND INDUSTRIALIZATION

- **Life test improvement**

As stated in the abstract, Quartz-S design was validated in 2022 during SELECTOR project.

Biggest challenge from this experience was the life testing as the product started to show some poor RF contact resistance measurement after 50 000 actuations shown in “Fig. 5”



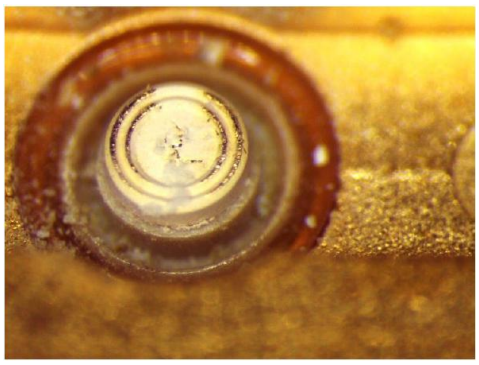


Fig. 5 Life test result and contact photograph after 1 000 000 actuations

After a lot of investigation and delta-testing, Radiall found a way to remove this white “residue” shown on the photo above and to have a unit compliant up to 300 000 actuations cycles.

- **Process improvement**

Radiall implemented and qualified a new equipment to deposit the correct quantity of glue on the RF contact and RF insulator. This process was previously made manually and highly dependent on the dexterity of the operator. “Fig. 6” shows a Ø 0.4 mm in diameter RF contact glued in its insulator.





Fig. 6 RF pin glue photograph and Automatic glue equipment

- **Screening RF measurement tools**

During SELECTOR, Radiall designed and improved a specific tool for a solderless RF measurement on screening unit. The unit is placed on a rigid plate and RF connection is made by solderless contact (Gold/Gold). The contact pressure is applied by a blade that act as a spring and keep the 50 Ohms impedance through the cavity.

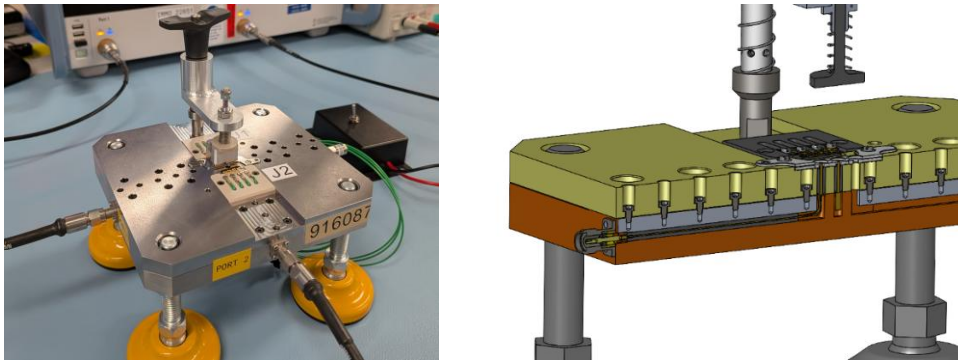


Fig. 7 RF measurement tool

ESA QPL QUALIFICATION CAMPAIGN

After all those changes were validated, Radiall was audited by ESA ESCC team in October 2025 (Report Radiall-AUD-2025). Findings are taking cared of and will be closed before end of 2026.

ESA qualification was launched in march 2026 as per ESCC3603[1]

Test	**Description**
Initial functional test	All RF and Electrical performance checked at Min and max temperature
Sine vibration test	30g up to 2000 Hz
Random vibration test	50 grms
Mechanical shock test	1500g Half sine 0.3ms
Thermal Vacuum test	25 cycles Non-Operating -55° to 95°C 10 cycles Operating -40 to 85°C
Operating life test	300 000 actuation cycles (-40°C to 85°C)
Final functional test	All RF and Electrical performance checked at Min and max temperature

Table 1. ESA QPL Test plan summary

For vibrations, the relays are fixed on a metallic plate that will vibrate at the specific ESA requirement. Radiall check first resonant frequency on each unit before and after each vibration test. No electrical or RF measurement are performed during test.

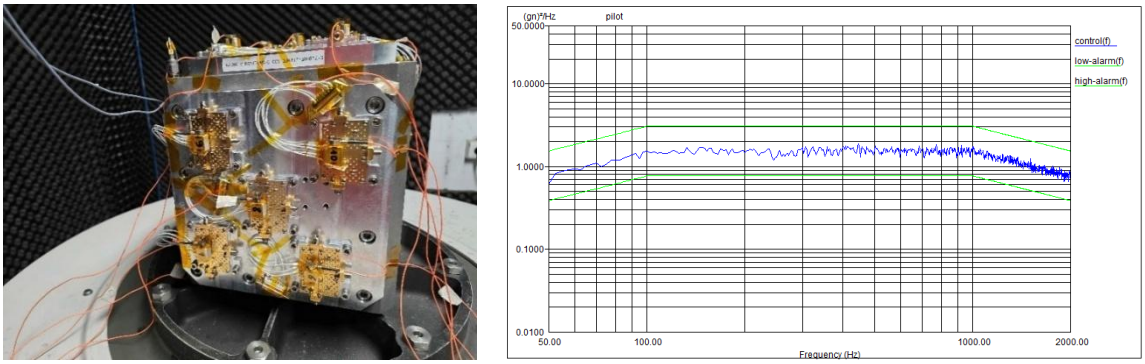


Fig. 8 Vibration test set-up & Random spectrum

Same principle for the shock testing with following shock applied:

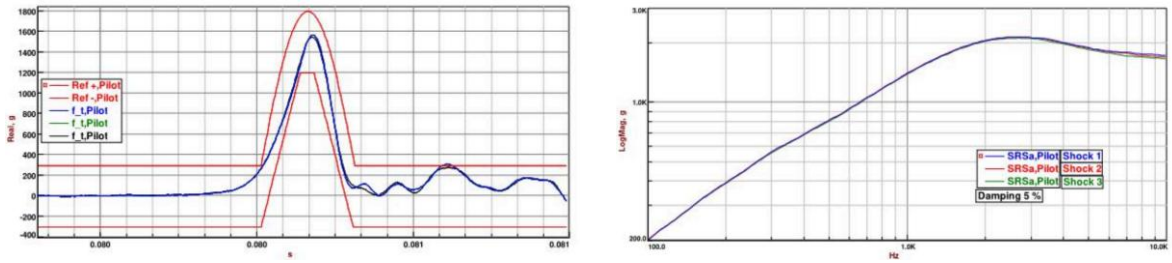


Fig. 9 Temporal Shock & SRS

Thermal Vacuum test is performed with a Thermal vacuum chamber (See "Fig. 10") that can reduce the pressure down to 1 x 10^{-6} mBar. The relays are placed inside the chamber, screwed on a Rigid plate for convection heat transfer and then placed under vacuum. The relays are also wired to an automatic bench to perform electrical measurement at each temperature plateau (Pick-up Voltage, switching time, RF path resistance, etc…). "Fig. 11" shows RF contact resistance measurement during TVT, 30 measurement at cold and hot temperature.

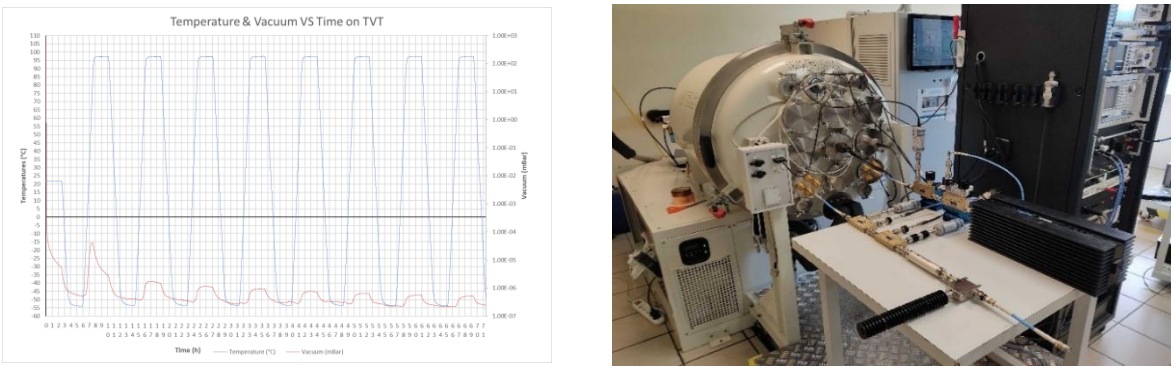


Fig. 10 Thermal Vacuum Chamber

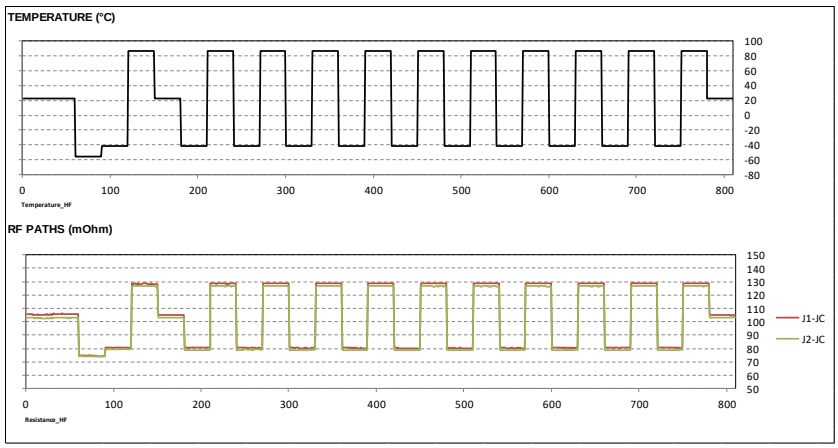


Fig. 11 Example of RF contact resistance measurement during TVT

CONCLUSION

Quartz-S ESCC QPL validation is planned for end of 2026.

With SELECTOR, TAS had the idea to implement the Quartz-S in their new Software-defined satellite soon to be launched with approximately 200 unit per satellite. This will be the first flight heritage for the Quartz-S.

Quartz-S was also proposed for other customer (with first EM and FM delivered) without any real hook yet due to major PCB design requirement to implement SMT relays to replace current electromechanical switches.

ACKNOWLEDGEMENT

Thanks to Leo Farhat, Joaquin Jimenez, Denis Lacombe, Jean-Luc Roux for their great support in the audit and the action that resulted.

REFERENCES

[1] [ESCC 3603 Issue 2]

[2] [ESCC 3603007 Issue 2]

Assessing Second-Life Supercapacitors in Space Systems: Towards an LCA Framework

Supercapacitors are attracting growing interest for space applications because of their high power density, long cycle life, and suitability for demanding operating conditions. At the same time, sustainability, circularity, and Zero Debris principles are becoming increasingly relevant in the early design of future space systems. Although life cycle assessment (LCA) studies on supercapacitor materials, manufacturing, and end-of-life are beginning to emerge, no dedicated LCA framework has yet been proposed for second-life supercapacitors, and this gap is even more pronounced for space-related applications.

This contribution proposes a preliminary, literature-based methodological framework to assess the environmental impacts and potential benefits of second-life supercapacitors in space systems. The approach builds on methodologies already developed for second-life lithium-ion batteries, in which collection, testing, transport, repurposing, reuse, and end-of-life are explicitly modelled and compared with direct replacement by new devices. In this work, that logic is extended to supercapacitors and discussed within the broader context of circular design strategies for space applications. Particular attention is given to the definition of first-life/second-life boundaries, allocation choices, additional impacts from transport and reprocessing, and avoided impacts associated with the substitution of newly manufactured devices. The framework is developed primarily from existing literature and publicly available data, including published LCA studies on supercapacitors, technical studies on supercapacitor degradation and second-life operation, and methodological references from battery second-life LCA.

Among the possible second-life pathways, the main focus is placed on the space-to-space scenario, as it is closely aligned with ESA's current Zero Debris ambitions and, more broadly, with the growing interest of space agencies in refurbishment, servicing, and circularity-oriented approaches for future space systems. This central case is complemented by two additional pathways, space-to-ground and ground-to-space, which are considered as comparative scenarios to discuss potential benefits, limitations, and methodological implications.

The aim of the work is not to provide a complete quantitative assessment of a validated case study, but rather to establish a structured basis for future investigations. Expected outcomes include the identification of the most relevant inventory elements, the definition of a transparent comparison structure between first-life and second-life supercapacitor use, and the mapping of the main knowledge gaps, methodological criticalities, and data requirements needed to support future quantitative studies and possible collaborative developments.

13-16 October 2026
ESA/ESTEC, Noordwijk, The Netherlands

GANDAIS Simon, PERARDEL Nicolas, PICCOT Jean-Marie
Nicomatic

Affiliation
Email: s.gandais@nicomatic.fr
Email: n.perardel@nicomatic.fr
Email: jm.piccot@nicomatic.fr

Managing Dynamic Separation Constraints: Case Study on Ground-to-Launcher Interconnections for Latitude's Micro-Launcher



Fig. 1. Latitude's Micro-Launcher

Abstract

The rise of "New Space" micro-launchers is driving ultra-fast development cycles while demanding absolute reliability during critical flight phases such as the release of ground-to-launcher connections (umbilicals). This article presents an innovative interconnection solution developed by Nicomatic for Latitude's launcher. Built on the modularity of the EN4165 standard, this custom system integrates floating mechanical compensation (±1 mm) and compatibility with the ejection mechanism. Validated for shocks up to 50g and temperatures ranging from -55°C to +125°C, this approach illustrates the weight optimization and reduced integration times required by today's industry.

1. Introduction: The New Space Paradigm and Nicomatic's Contribution

The emergence of small satellite (SmallSat) constellations has stimulated the development of agile, cost-effective micro-launchers. The French launcher, developed by Latitude (19 meters high, 23 tons at liftoff, with a payload capacity of 200 kg), is targeting an ambitious industrial pace, with a goal of one launch per week by 2030.

To support such a launch rate, critical interconnection systems must break free from the constraints of traditional space-grade components (mass, footprint, extremely long ESCC qualification cycles) without compromising reliability in any way. Recognized for its expertise in interconnection solutions designed for harsh environments, Nicomatic was asked to develop a ground-to-launcher electrical separation connection capable of being integrated quickly while withstanding the extreme dynamic stresses of liftoff.

2. Design Challenge: Geometrical and Weight Optimization

In conventional space design, circular standards (such as MIL-DTL-38999) are often used to ensure robust connections.

However, the specifications of a micro-launcher impose specific constraints at the umbilical separation panels: the available surface area is extremely limited. Using several circular receptacles side by side to distribute the various lines (power and signal) creates a restrictive surface footprint.

To address this geometrical constraint, Nicomatic's engineering team turned to an adaptation of the EN4165 aeronautical standard. Its rectangular geometry makes it possible to optimize packaging on flat bulkheads. In addition, its modular design allows power and signal modules to be grouped within one single panel (up to 12 cavities). This provides a drastic space saving and reduces the overall mass of the interface.



Fig. 2. One of the solutions implemented by Nicomatic based on the EN 4165 standard

Design Criterion	Circular Approach (Standard D38999-Type)	Modular Rectangular Approach (Selected EN4165 Solution)	Direct Benefit for the Umbilical Panel
Power & Signal Line Management	Use of several dedicated connectors or specific fixed inserts.	Native mixing of power and signal within one single panel (up to 12 cavities).	Reduced number of connectors to manage during release kinematics.
Form Factor and Footprint	Circular: excellent for the robustness of isolated cable connections, but requires radial spacing on a panel.	Rectangular: "Rack & Panel" format enabling high-density stacking.	Maximum optimization of the available surface on the launcher's separation plates.
Materials and Weight	Often available in stainless steel or aluminum for launch environments.	Nickel-plated aluminum body with ultra-light rear accessories (backshells).	Targeted weight reduction on the separation interface, which is critical for payload performance.
Mechanical Separation Management	Conventional release using a *lanyard release* system.	Custom panel integrating a floating compensation mechanism (±1 mm) and rapid ejection.	Absorbs vibrations (50g) and enables smooth separation matching the rocket opening sequence.

3. Engineering the Ground-to-Onboard Separation System

The ground-to-launcher connection is subjected to major dynamic stresses (acoustic, vibrational, and thermal) just before and during liftoff. The solution required the design of custom plates (*Rack & Panel* format) integrating two key mechanisms.

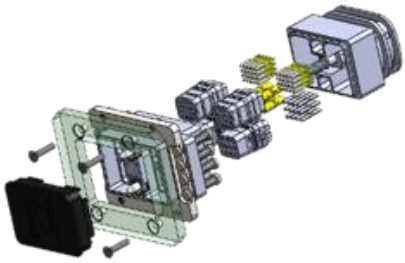


Fig. 3. Exploded view of the solution

3.1. The Mechanical Compensation System (Floating System)

At engine ignition, the structure undergoes intense deformation and vibration. A rigid connection would risk transmitting these stresses to the contacts, causing fretting corrosion or micro-interruptions.

To overcome this issue, the EN4165 plates incorporate a three-dimensional compensation system along the Ox, Oy, and Oz axes. This mechanism can absorb misalignments of up to ±1 mm, thus preserving signal integrity without transmitting mechanical stress. To optimize weight, the connector bodies are made of nickel-plated aluminum and paired with ultra-light backshells.

3.2. The Quick Disconnect Mechanism

A launcher umbilical requires a high retention force during the preparation phase. The team therefore developed a stainless steel rapid ejection mechanism. This releasable system precisely follows the rocket's opening sequence and kinematics at liftoff, ensuring a clean separation and preventing any risk of jamming.



Fig. 4. One of the solutions implemented by Nicomatic based on the EN 4165 standard

4. Validation Data (New Space Test Campaign)

In line with the New Space philosophy, qualification was targeted to the exact mission profile in order to reduce costs and lead times, avoiding the burden of a generic ESCC qualification.

- **Vibration and Shock:** The connector maintained perfect signal continuity during vibration tests up to **50g**, simulating the mechanical stress of liftoff and flight.
- **Thermal Constraints:** The materials ensure full operability over a temperature range of **55°C to +125°C**.

5. The Critical Challenge: Reducing Development Time

Beyond performance, the major innovation of this project lies in *time-to-market* optimization. The on-site *co-engineering* approach made it possible to validate the concept in a sprint lasting only a few days. In addition, hardware integration time on the rocket is optimized through the design of quick fastening systems and native keying features (EN4165 polarization nuts), limiting human error during assembly.

6. Conclusion

This case study demonstrates that Nicomatic's expertise, combining a reliable modular rectangular standard (EN4165) with custom mechanical engineering (floating compensation and quick ejection), can solve complex physical challenges. This solution therefore stands out as a pragmatic response to the New Space industry's need for reduced weight, optimized use of space, and rapid integration.

Towards Green and Sustainable Supercapacitors for Space-Grade Electrode Processing

Veronika Šedajová, Tomáš Zedníček

ATOMIVER s.r.o., Lanskroun, Czech Republic
Corresponding author: tom@atomiver.com

ABSTRACT

Supercapacitors are attractive for aerospace and other high-reliability applications because they can deliver high power, support ultrafast charging, and survive very long cycle life. However, the manufacturing route for high-performance carbon-based electrodes still depends heavily on N-methyl-2-pyrrolidone (NMP), a toxic solvent that is increasingly constrained by environmental and occupational regulations. In this work, we demonstrate a practical route toward greener supercapacitor manufacturing by replacing NMP with two alternative solvents, Cyrene and Tamisolve, while maintaining industrially relevant electrode quality and electrochemical performance. The active material is a nitrogen-doped graphene derivative, SC-GN3, processed with either polyvinylidene fluoride (PVDF) or polyvinylpyrrolidone (PVP) binders. High-mass-loading electrodes above 6 mg cm^{-2} were fabricated on carbon-coated aluminium current collectors and tested in symmetric two-electrode devices. The best-performing green formulation, PVDF–Cyrene, achieved 152 F g^{-1} at 1 A g^{-1}, energy density of 66.6 Wh kg^{-1} at 1.85 kW kg^{-1}, and 91% capacitance retention after 100,000 cycles. PVP–Cyrene provided a fluorine-free alternative with 133 F g^{-1}, 64.2 Wh kg^{-1}, and 78% retention. Bending and tape-adhesion tests confirmed that Cyrene-processed electrodes can combine high loading with robust film integrity. The results indicate that green solvent systems can replace NMP in advanced supercapacitor processing without compromising performance, while improving the environmental profile of electrode manufacturing.

Keywords: supercapacitor, nitrogen-doped graphene, green solvents, Cyrene, Tamisolve, PVDF, PVP, space manufacturing

1. INTRODUCTION

Supercapacitors are increasingly relevant to aerospace and other high-reliability power systems because they offer fast charge and discharge, high power density, and long operational lifetime. These attributes make them useful for peak-power buffering, pulsed loads, launch and landing support systems, and hybrid energy storage architectures where reliability and predictable response are essential. For space-sector engineers, the key question is not only whether a device performs well in the laboratory, but whether it can be manufactured in a way that is scalable, robust, and compatible with long-term industrial constraints.

One of the main bottlenecks in carbon-electrode manufacturing is the widespread use of N-methyl-2-pyrrolidone (NMP) in slurry processing. NMP disperses carbon powders and polymer binders efficiently, but it is also a toxic solvent that faces tighter regulatory control in Europe and the United States. From a production perspective, this creates challenges in handling, emissions control, worker safety, and future compliance. For this reason, there is strong motivation to identify solvents that are less hazardous while still delivering the film quality, adhesion, and electrochemical performance required for high-rate energy-storage devices.

This paper addresses that challenge by comparing NMP with two greener solvents, Cyrene and Tamisolve, in the processing of nitrogen-doped graphene supercapacitor electrodes. Cyrene is a biomass-derived solvent with a favorable environmental profile, whereas Tamisolve is a low-toxicity dipolar aprotic solvent developed as a replacement for NMP in polymer processing. We evaluate their compatibility with two binders: PVDF, the conventional fluorinated binder used in many electrode systems, and PVP, a more environmentally benign non-fluorinated binder. The objective is to determine whether green solvent systems can sustain high mass loading, strong adhesion to current collectors, and long-term cycling stability at the level expected for advanced applications.

The work is based on a scaled-up synthesis of SC-GN3, a nitrogen-doped graphene derivative with high nitrogen content and favorable electrochemical properties. The study combines materials characterization, electrode processing, electrochemical testing, and mechanical integrity assessment. In addition to reporting electrochemical performance, we focus on manufacturability metrics that are often underreported but critical for transferring a formulation from laboratory scale to production scale.

2. MATERIALS AND METHODS

2.1 Active Material

The active material used in this work was SC-GN3, a nitrogen-doped graphene derivative produced by a large-scale synthesis route based on a 100 g batch. The material was subjected to quality control before electrode fabrication. X-ray photoelectron spectroscopy confirmed a nitrogen content reaching 16.2 at.%, which is consistent with the expected composition of the material. Structural analysis by SEM, FTIR, and Raman spectroscopy confirmed the multilayer graphene morphology, the presence of heteroatom-related functionalities, and a defect-rich but conductive carbon network (Fig. 1).

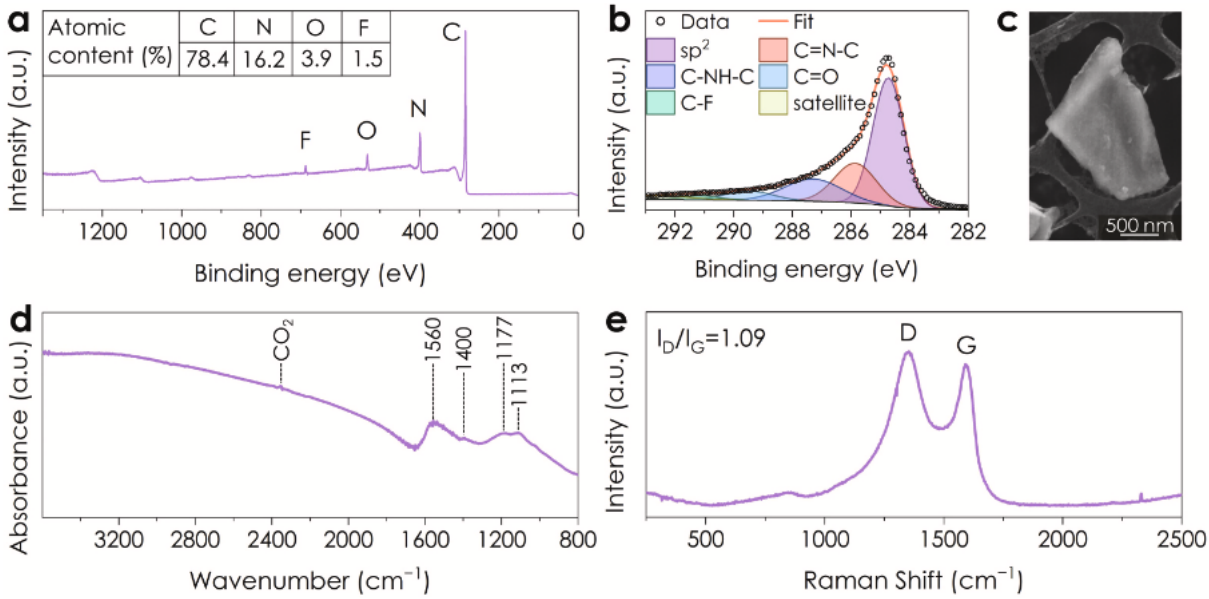


Fig. 1. (a) XPS Survey spectrum of SC-GN3. (b) Deconvolution of the XPS spectrum for the C1s regions of SC-GN3. (c) SEM image of SC-GN3 particle. (d) FTIR spectrum of SC-GN3. (e) Raman spectrum of SC-GN3.

Comparison of selected properties of tested solvents.

Solvent	Boiling point (°C)	Surface tension (mN m^{-1} at 25 °C)	Viscosity at 25 °C (mPa s)	Flash point (°C)	Price (EUR/L)*	Application challenges
NMP	202	41	1.7	91	49	Toxic, hazardous, and usage restrictions
Cyrene	226	72.5	15	108	317	Poor adhesion, solvability issues with PVDF
Tamisolve	241	67.3	4	108	79	No data available

* price quotation per 1 L volumes from Carl Roth (6/2025).

Table 1. Comparison of selected properties of tested solvents

The combination of high nitrogen doping and surface functionality is beneficial for supercapacitor electrodes because it improves wetting, promotes stable dispersions in polar media, and supports efficient ion access at the electrode/electrolyte interface. In practical terms, these properties reduce the risk of agglomeration during slurry processing and improve the uniformity of the final coating.

2.2 Solvents and Binders

Three solvent systems were compared: NMP, Cyrene, and Tamisolve. NMP was used as the baseline because it remains a standard processing solvent in carbon-based electrode manufacturing. Cyrene was selected as a green, bio-based solvent, and Tamisolve was chosen as a lower-toxicity alternative with physical properties closer to NMP.

Two binders were evaluated. PVDF was used as the conventional binder due to its established use in electrochemical electrodes and its mechanical strength after drying. PVP was used as a non-fluorinated alternative to evaluate whether a

more environmentally benign binder can be introduced without excessive loss of performance. Solubility screening showed that NMP dissolved both binders readily, Cyrene dissolved PVP well but required elevated temperature for complete PVDF dissolution, and Tamisolve provided good compatibility with both binders (Fig. 2).

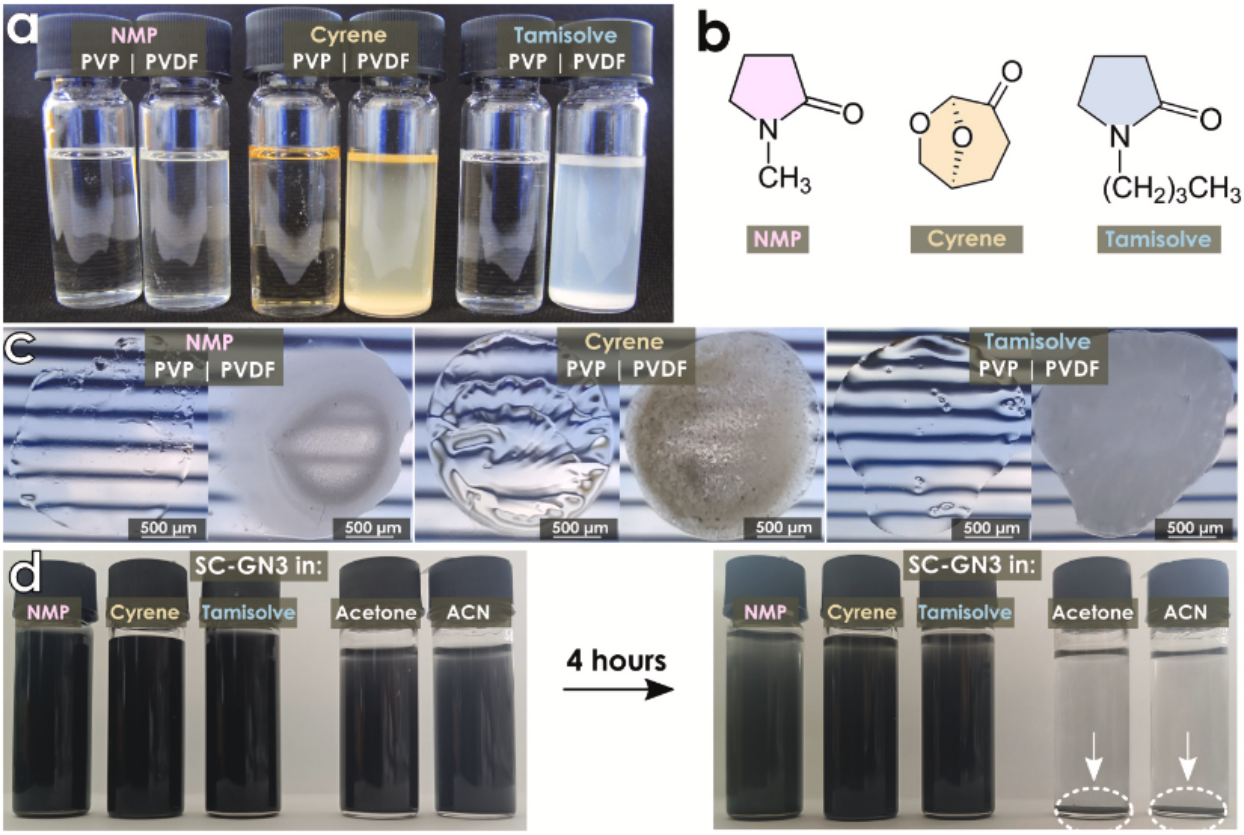


Fig.2. Comparison of binder solubility and slurry stability in NMP, Cyrene, and Tamisolve. (a) Solubility of binders in solvents. From left: PVP or PVDF in NMP, PVP or PVDF in Cyrene, PVP or PVDF in Tamisolve. (b) Structural formula of NMP, Cyrene and Tamisolve solvents. (c) Photographs of dried binder films on a glass slide. (d) Dispersion of SC-GN3 in NMP, Cyrene, Tamisolve, Acetone, and ACN before and after 4h, showing sedimentation in Acetone and ACN solutions.

2.3 Electrode Fabrication

Electrodes were prepared with a fixed formulation of 87 wt% SC-GN3, 3 wt% binder, and 10 wt% conductive carbon. The binder was first dissolved in the selected solvent, then mixed with conductive additive and active material to obtain a paste-like slurry. The slurry was homogenized by vortex mixing and planetary mixing, followed by sonication to improve dispersion quality. The material was then coated onto carbon-coated aluminium foil using a doctor blade, dried under vacuum, calendared, and punched into discs for device assembly.

The total mass loading per electrode was maintained in the range of 15.8 to 18 mg, corresponding to approximately 6.2 to 7.1 mg cm^{-2}. This is an important point for the SPCD audience because high-mass-loading electrodes are much closer to practical device requirements than the thin coatings often used in exploratory studies.

2.4 Device Assembly and Testing

Symmetric two-electrode supercapacitor cells were assembled using glass microfiber separators and a mixed electrolyte based on ionic-liquid and organic-solvent components. The device was compressed in a standard cell holder and tested by galvanostatic charge-discharge, cyclic voltammetry, and electrochemical impedance spectroscopy. Cycling stability was assessed over 100,000 cycles at 10 A g^{-1}, and capacitance retention was tracked over the full test window.

Specific capacitance, energy density, power density, and equivalent series resistance were calculated from the charge-discharge data using standard equations for full-cell evaluation. In addition to electrochemical tests, the electrodes were evaluated mechanically using bending tests and a tape-based grid adhesion test adapted from ASTM D3359. These mechanical tests were selected because they provide practical indicators of whether the films can survive coating, handling, and winding operations.

3. RESULTS AND DISCUSSION

3.1 Material Quality and Dispersion Behavior

The SC-GN3 material exhibited the expected graphene-like morphology and a highly doped carbon structure. XPS analysis confirmed substantial nitrogen incorporation, while Raman spectroscopy showed a D/G ratio of 1.09, indicating a defect-rich structure with preserved conductivity. For supercapacitor applications, this combination is attractive because it supports strong interfacial charge storage while maintaining electronic transport across the electrode film.

Dispersion behavior was also favorable. SC-GN3 formed stable suspensions in all three solvents over several hours, with no significant sedimentation observed. This is a useful process indicator because a stable slurry is a prerequisite for uniform coating, consistent porosity, and repeatable device performance. By contrast, acetone and acetonitrile showed rapid sedimentation and were not suitable for this application.

3.2 Solvent and Binder Compatibility

The most direct processing result was that Cyrene and Tamisolve can replace NMP without losing the ability to prepare usable high-loading electrodes. NMP remained the easiest solvent for PVDF and PVP dissolution, but Cyrene and Tamisolve offered clear environmental advantages. Cyrene required elevated temperature to fully dissolve PVDF, reflecting a processing trade-off rather than a fundamental limitation. Tamisolve showed better compatibility with PVDF than Cyrene and also dissolved PVP well.

A practical observation is that the choice of binder strongly affects film formation. PVDF produced mechanically strong films, while PVP tended to form more uniform and flexible films, particularly in Cyrene. However, PVP also introduced some limitations in adhesion, which must be considered if the electrode is intended for high-stress cell formats. This reinforces the idea that sustainability improvements must be balanced against manufacturing requirements.

3.3 Electrochemical Performance

Electrochemical testing showed that the conventional PVDF–NMP system delivered 131 F g^{-1} at 1 A g^{-1}. Replacing NMP with Cyrene improved performance rather than degrading it. The PVDF–Cyrene formulation achieved 152 F g^{-1} and the lowest ESR among the tested systems, at 6.9 to 7.1 ohms depending on the evaluation point. PVDF–Tamisolve also performed well, reaching 140 F g^{-1}.

Mixture	Binder	Solvent	Capacitance in two-electrode setup (F g^{-1})	Total mass loading (mg)	Mass loading (mg cm^{-2})	ESR (Ω)
87 % SC-GN3 + 3 % binder + 10 % Timcal	PVDF	NMP	131	32.6	6.4	9.8
	PVDF	Cyrene	152	31.5	6.2	6.9
	PVDF	Tamisolve	140	31.6	6.2	10.2
	PVP	NMP	117	36.2	7.1	7.9
	PVP	Cyrene	133	32.7	6.4	7.1
	PVP	Tamisolve	–	–	–	–

Table 2. The effect of solvent and binder combination on gravimetric capacitance. The capacitance was calculated from GCD cycle recorded at the current density of 1A g^{-1}

The galvanostatic charge-discharge curves, cyclic voltammetry, Nyquist plots, and cycling stability are shown in **Fig. 3**.

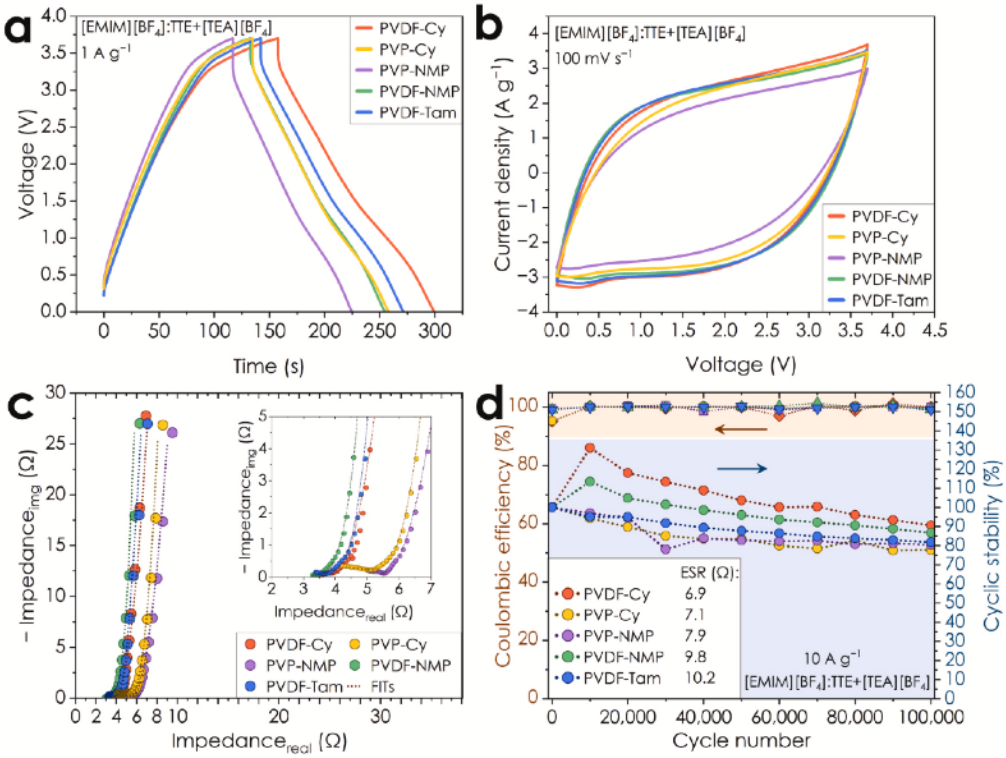


Fig.3. Electrochemical response of SC-GN3-based supercapacitor electrodes prepared with different solvent-binder combinations. (a) GCD profiles of SC-GN3 mixtures at 1 A g-1. Combination of PVDF-Cy (red), PVP-Cy (yellow), PVP-NMP (violet), PVDF-NMP (green), PVDF-Tamisolve (blue). (b) Cyclic voltammetry profiles at 100 mV s-1. (c) Nyquist plot with close-up inset. (d) Cyclic stability for 100,000 cycles at 10 A g-1 (right) with Coulombic efficiency (left).

The PVP-based systems showed that fluorine-free processing is possible, although with some performance trade-offs. PVP–Cyrene achieved 133 F g^{-1}, 64.2 Wh kg^{-1}, and 1.80 kW kg^{-1}. In contrast, PVP–Tamisolve was not suitable for electrochemical testing because the film did not adhere sufficiently to the substrate. This result is important because it shows that green solvent selection alone is not enough; solvent-binder-current-collector compatibility must be engineered as a system.

The GCD curves retained the expected triangular shape of electric double-layer capacitors, with only modest IR drop. CV profiles were close to rectangular, without strong redox peaks, indicating that the charge-storage mechanism is dominated by double-layer behavior rather than fast faradaic redox reactions. This is consistent with high-surface-area carbon electrodes tested under conditions where transport limitations become more pronounced as the mass loading increases.

3.4 Long-Term Cycling Stability

Long-term cycling was particularly encouraging for PVDF–Cyrene, which retained 91% of its capacitance after 100,000 cycles at 10 A g^{-1}. That level of stability is a strong sign that the green solvent does not compromise interfacial stability or electrode cohesion during repeated high-rate operation. PVDF–Tamisolve also remained durable, with 82% retention after the same test duration.

The lower retention of PVP–Cyrene, at 78%, suggests that binder chemistry matters as much as solvent selection. A likely explanation is the combination of PVP's hydrophilicity and possible interactions with the electrolyte under a wide voltage window. While the exact degradation mechanism would require deeper post-mortem analysis, the result is still informative because it delineates the processing window where fluorine-free binders are viable and where they may need additional optimization.

3.5 Mechanical Integrity and Adhesion

Mechanical tests confirmed that the green solvent systems are not only electrochemically viable, but also mechanically robust. Bending around a 180-degree radius showed that PVDF-based films processed with Cyrene and Tamisolve remained strongly attached to the carbon-coated aluminium current collector, although they were somewhat more prone to cracking than PVP-based films. Repeated bending caused only a modest increase in resistance, indicating that the electrode/current-collector interface remained intact.

Mechanical flexibility and crack resistance after bending around a 180° rod are illustrated in **Fig. 4**.

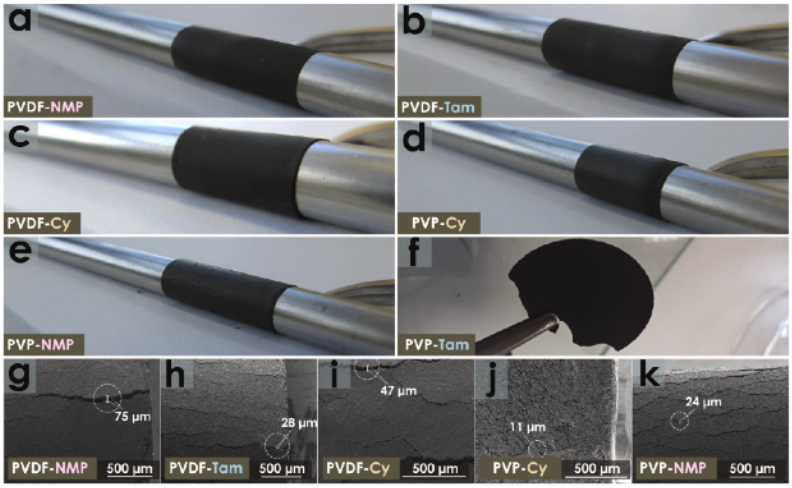


Fig.4. Mechanical flexibility and crack resistance of high-mass-loading electrodes after bending around a 180° stainless-steel rod. The figure compares PVDF- and PVP-based films processed with NMP, Cyrene, and Tamisolve. The width of each film is >1 cm. (a) PVDF-NMP, (b) PVDF-Tam, (c) PVDF-Cy, (d) PVP-Cy, (e) PVP-NMP, (f) PVP-Tam free-standing film. SEM images of films were taken during the bending position: (g) PVDF-NMP, (h) PVDF-Tam, (i) PVDF-Cy, (j) PVP-Cy, (k) PVP-NMP.

Adhesion and cohesion under increasing tape force are summarized in **Fig. 5**.

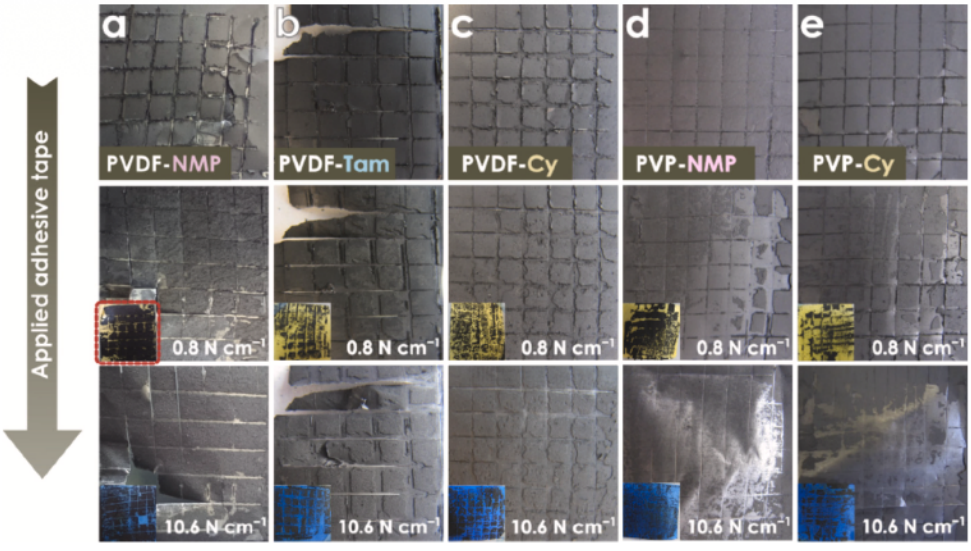


Fig.5. Tape-based grid adhesion test of electrode films prepared on carbon-coated aluminium foil. The figure shows adhesion and cohesion behavior under increasing tape force, highlighting the superior adhesion of Cyrene-based PVDF electrodes.4 tapes were applied in the same order for every sample. (a) PVDF-NMP, (b) PVDF-Tam, (c) PVDF-Cy, (d) PVP-NMP, (e) PVP-Cy. Tapes were used on every sample in the same order as follows: 0.8 N cm^{-1}, 1.15 N cm^{-1}, 2.6 N cm^{-1}, 10.6 Ncm^{-1}. Insets: The used adhesion tape shows residues of the removed electrode film.

The adhesion-grid test provided an additional industrially relevant metric. PVDF–Cyrene and PVDF–Tamisolve showed strong adhesion and cohesion even under aggressive tape forces, while PVDF–NMP showed weaker cohesion and more material removal. PVP–Cyrene bent well and showed fewer cracks, but its adhesion to the substrate was weaker. This means that PVP–Cyrene may be better suited to low-stress, flexible architectures, while PVDF–Cyrene is more suitable for winding and mechanically demanding formats.

3.6 Implications for Space-Grade Manufacturing

For space-sector engineers, the main lesson is that greener processing does not have to mean lower-performance electrodes. In fact, the best green formulation in this study, PVDF–Cyrene, outperformed the conventional PVDF–NMP reference while also improving long-term retention and mechanical integrity. That is significant because aerospace applications typically place equal weight on performance, manufacturability, and reliability.

A second important implication is that the electrode film can be made at practical mass loadings on industry-standard carbon-coated aluminium foil. This suggests compatibility with scalable coating and calendaring routes, which are the kinds of manufacturing steps relevant to serial production. The combination of high loading, strong adhesion, and long-term stability is therefore more important than any single headline capacitance value.

4. CONCLUSIONS

This study demonstrates that NMP can be replaced by greener solvents, especially Cyrene and Tamisolve, in the fabrication of high-performance supercapacitor electrodes based on nitrogen-doped graphene. The most successful formulation, PVDF–Cyrene, achieved 152 F g^{-1} at 1 A g^{-1}, 66.6 Wh kg^{-1}, 1.85 kW kg^{-1}, and 91% capacitance retention after 100,000 cycles, while maintaining high mass loading and strong adhesion to carbon-coated aluminium current collectors.

PVP–Cyrene provided a fluorine-free processing route with competitive performance and excellent flexibility, although adhesion and long-term retention were lower than in the PVDF-based system. Tamisolve also proved to be a valid replacement for NMP, especially with PVDF, and offers a useful alternative where process constraints favor a solvent with NMP-like handling characteristics.

Overall, the results show that greener solvent systems can support robust and scalable manufacturing of advanced supercapacitor electrodes. For the SPCD community, the main message is that sustainable processing is not merely an environmental preference; it can also be a technically sound route toward reliable high-performance energy-storage components for space and other demanding applications.

ACKNOWLEDGEMENT

This work is based on supported activities by the European Union's Horizon Europe EIC Transition project Trans2Dchem (No. 101057616). The authors used Artificial Intelligence language models only to improve the clarity and fluency of the manuscript. The authors carefully edited the content afterwards.

CONFLICT OF INTEREST

The authors declare that there are no conflicts of interest regarding the publication of this work.

REFERENCES

[1] M. Salanne, B. Rotenberg, K. Naoi, K. Kaneko, P.-L. Taberna, C.P. Grey, B. Dunn, P. Simon, Efficient storage mechanisms for building better supercapacitors, Nat. Energy 1 (2016) 1–10. https://doi.org/10.1038/ nenergy.2016.70.

[2] I. Dědek, V. Šedajová, V. Kupka, T. Zedníček, L. Primavesi, D. Aurbach, M. Noked, M. Otyepka, High-Performance Carbon-Based Supercapacitors, 2D Mater. (2025). https://doi.org/10.1088/2053-1583/adf653.

[3] P. Ruschhaupt, A. Varzi, S. Passerini, Natural Polymers as Green Binders for High-Loading Supercapacitor Electrodes, ChemSusChem 13 (2020) 763–770. https://doi.org/10.1002/cssc.201902863.

[4] Z. Du, K.M. Rollag, J. Li, S.J. An, M. Wood, Y. Sheng, P.P. Mukherjee, C. Daniel, D.L. Wood, Enabling aqueous processing for crack-free thick electrodes, J. Power Sources 354 (2017) 200–206. https://doi.org/10.1016/j.jpowsour.2017.04.030.

[5] K. Rollag, D. Juarez-Robles, Z. Du, D.L. Wood, P.P. Mukherjee, Drying Temperature and Capillarity-Driven Crack Formation in Aqueous Processing of Li-Ion Battery Electrodes, ACS Appl. Energy Mater. 2 (2019) 4464–4476. https://doi.org/10.1021/acsaem.9b00704.

[6] N.A. Stini, P.L. Gkizis, C.G. Kokotos, Cyrene: a bio-based novel and sustainable solvent for organic synthesis, Green Chem. 24 (2022) 6435–6449. https://doi.org/10.1039/D2GC02332F.

[7] R. Poon, I. Zhitomirsky, Application of Cyrene as a solvent and dispersing agent for fabrication of Mn3O4-carbon nanotube supercapacitor electrodes, Colloid Interface Sci. Commun. 34 (2020) 100226. https://doi.org/10.1016/j.colcom.2019.100226.

[8] J. Wang, T. Yang, A.A. Obisanya, Y. Ma, Z. Ren, X. Tan, W. Lei, A. Song, F. Gao, Force-Field Regulation Engineered Heterogeneous Graphene Micro-Aerogels as Versatile Platforms for High-Mass-Loading Energy Storage, Adv. Energy Mater. 15 (2025) 2500992. https://doi.org/10.1002/aenm.202500992.

[9] W. Tian, P. Ren, X. Hou, Z. Guo, R. Xue, Z. Chen, Y. Jin, Biomass derived N/O self-doped porous carbon for advanced supercapacitor electrodes, Ind. Crops Prod. 202 (2023) 117032. https://doi.org/10.1016/j.indcrop.2023.117032.

[10] Y. Niu, M. Guo, Y. Zhang, J. Yang, X. Zhang, Y. Gao, X. Wang, L. Sheng, J. Shi, Heteroatom-doped layered hierarchical porous carbon electrodes with high mass loadings for high-performance supercapacitors, J. Energy Storage 73 (2023) 109064. https://doi.org/10.1016/j.est.2023.109064.

[11] T. Lv, X. Yang, Y. Zhang, X. Wang, J. Qiu, Fabrication of Soft-Hard Heterostructure Porous Carbon with Enhanced Performance for High Mass-Loading Aqueous Supercapacitors, Small 20 (2024) 2310645. https://doi.org/10.1002/smll.202310645.

[12] C. Li, X. Li, Q. Yang, L. Wu, C. Wang, H. Tian, C. Wang, X. Chen, J. Shao, Vascular System Inspired 3D Electrolyte Network for High Rate and High Mass Loading Graphene Supercapacitor, Adv. Funct. Mater. 34 (2024) 2315137. https://doi.org/10.1002/adfm.202315137.

[13] V. Šedajová, A. Bakandritsos, P. Błoński, M. Medveď, R. Langer, D. Zaoralová, J. Ugolotti, J. Dzíbelová, P. Jakubec, V. Kupka, M. Otyepka, Nitrogen doped graphene with diamond-like bonds achieves unprecedented energy density at high power in a symmetric sustainable supercapacitor, Energy Environ. Sci. 15 (2022) 740–748. https://doi.org/10.1039/D1EE02234B.

[14] I. Dědek, V. Kupka, V. Šedajová, P. Jakubec, M. Navrátil, M. Otyepka, Toward transitioning to green and sustainable supercapacitors, Chem. Eng. J. 529 (2026) 172220. https://doi.org/10.1016/j.cej.2025.172220.